Mechanical Properties of Helical and Mesomorphic Forms of Syndiotactic Polypropylene at Different Temperatures

Claudio De Rosa, Odda Ruiz de Ballesteros,* and Finizia Auriemma

Dipartimento di Chimica, Università di Napoli "Federico II", Complesso Monte S. Angelo, Via Cintia, 80126 Napoli, Italy

Received April 22, 2004; Revised Manuscript Received June 15, 2004

ABSTRACT: A parallel analysis of the polymorphic behavior and mechanical properties of syndiotactic polypropylene samples with different stereoregularity and crystallized in the helical form and in the trans-planar mesomorphic form, stretched at room temperature and at 4 °C, is reported. Oriented fibers show good elastic properties at room temperature, regardless of the crystalline form present in the original fiber. The elastic behavior is associated with reversible polymorphic transitions occurring in the crystalline regions during the stretching and relaxation of fibers. The helical form or trans-planar mesomorphic form present in the fibers transform by stretching into the form III, which transforms back into the helical or trans-planar mesomorphic forms by removing the tension. At 4 °C fibers in trans-planar mesomorphic form do not transform into the form III by stretching, and no phase transition is observed upon releasing the tension. Correspondingly, the elastic recovery at 4 °C of mesomorphic fibers is significantly reduced in a very small deformation range. These results indicate that both the enthalpic effect, due to the polymorphic transition occurring in the crystals, and the entropic effect, due to the conformational transitions of the amorphous tie chains, contribute simultaneously to the elastic recovery of syndiotactic polypropylene fibers.

Introduction

Syndiotactic polypropylene (s-PP) represents an unusual example of highly crystalline thermoplastic material with a relatively high glass transition temperature ($T_g \approx 0$ °C), showing unexpected elastic properties.[1−4] More precisely, unoriented compression-molded samples of s-PP, generally crystallized in the most stable form I[5,6] with chains in s(2/1)2 helical conformation, undergo plastic deformation upon stretching and show poorly elastic properties. The crystalline domains tend to assume preferred orientation along the stretching direction and a phase transition from the helical form I into the trans-planar form III[7,8] of s-PP gradually occurs. Form III is unstable in unstrained samples and transforms into the more stable helical form II upon removing the tension in stretched fibers.[2,3,9−12] The crystalline orientation is preserved in the relaxed fibers, and only a small recovery of the initial dimensions of specimens is observed.[2−4]

On the contrary, strained and stress-relaxed fibers of s-PP present very good elastic properties, showing a nearly total recovery of the initial dimensions of the specimens upon successive stretching and relaxation cycles.[1−4] In highly crystalline fibers stretched at room temperature, the crystalline helical form II present in the stress-relaxed fiber transforms by stretching into the crystalline trans-planar form III, which transforms back into the helical form II after releasing the tension.[2,10,12] It has been suggested that this reversible crystal−crystal phase transition is related to the elastic behavior of s-PP.[2,3,12] This hypothesis is supported by the fact that when the formation of the trans-planar form III by stretching is inhibited, as in the case of stereo- and regioirregular s-PP produced by traditional Ziegler−Natta vanadium-based catalysts[2,10] or s-PP samples stretched at temperature higher than 60 °C,[3] the elastic properties are lost. Therefore, contrary to the common thermoplastic elastomers, the elastic behavior of s-PP fibers seems to be characterized by an enthalpic contribution and related to a crystal−crystal reversible phase transition.[2,3,12] An entropic effect, due to the chains in the amorphous regions, which tend to restore the disordered random coil conformation, also contributes to the elastic recovery.[1−4]

The role played by the enthalpic and entropic contributions on the elastic behavior of s-PP depends on the degree of crystallinity and stereoregularity of the s-PP sample.

Recently, the mechanical properties and elastic behavior of high-molecular-weight low syndiotactic polypropylene samples, prepared with catalysts of new design based on "constrained geometry" complexes of titanium, have been described.[13,14] Contrary to highly stereoregular and crystalline s-PP, low syndiotactic samples present good elastic properties even for unoriented compression-molded films, showing a nearly total recovery of the initial dimensions already after the first stretching.[14a] Because of the very low crystallinity, these samples experience a negligible irreversible plastic deformation and behave like typical thermoplastic elastomers in which the small crystalline domains act as physical knots in a prevailing amorphous matrix, preventing the viscous flow of the chains. In this case the entropic effect due to the conformational transition of the amorphous chains, which connect as tie chains the crystalline domains, is mainly responsible for the elastic behavior.[13,14] A reversible phase transition between the mesomorphic form[15−17] of s-PP with chains in the trans-planar conformation and the helical form I, occurring in the crystalline regions during successive stretching and relaxation, provides an enthalpic contribution which assists the elastic recovery of the samples.[14]

* Corresponding author: Tel ++39 081 674448; Fax ++39 081 674090; e-mail odda.ruizdeballesteros@unina.it.

10.1021/ma049214h CCC: $27.50
Published on Web 09/03/2004

Table 1. Fully Syndiotactic Pentad Contents ([*rrrr*]), Molecular Weights (M_w), Indices of Polydispersity (M_w/M_n), and Melting Temperatures (T_m) of the Samples sPP1 and sPP2

sample	[*rrrr*] (%)	M_w	M_w/M_n	T_m (°C)[a]
sPP1	93	2.13×10^5	2.4	149
sPP2	78	1.93×10^5	4.5	124

[a] Measured on the polymer powders with a differential scanning calorimeter (Perkin-Elmer DSC7) in a flowing N_2 atmosphere at a heating rate of 10 °C/min.

These studies have indicated that the physical and mechanical properties of s-PP are strongly influenced by the complex polymorphism, which in turn depends on many parameters, as the stereoregularity of the polymer samples,[2,9,12−14,17] the experimental conditions (i.e., stretching temperature),[3,18] and also the crystalline modification of the starting materials.[18] It has been, indeed, recently shown that the memory of the crystalline forms initially present in the unoriented s-PP samples, and of those formed during stretching, has a relevant effect on the structural transitions occurring in stretched and stress-relaxed fibers.[18] In particular, the metastable trans-planar form III, obtained by stretching samples initially in the helical form or in the trans-planar mesomorphic form, transforms into the crystalline forms present in the unoriented sample or formed during the stretching, when the tension is released.[18,19] These data indicate that the structural evolution of the trans-planar form III upon removing the tension in stretched fibers depends on the memory of the crystalline forms present in the unoriented materials and on the memory of the crystalline forms produced during the stretching.[18]

In the hypothesis that the elastic behavior of s-PP fibers is related to the structural evolution of the trans-planar form III, it is expected that the elastic properties are affected by the same parameters that influence the structural transitions.

In this paper the mechanical properties and the elastic behavior of s-PP samples having different stereoregularity and crystallized in different polymorphic modifications are analyzed. The mechanical analysis has been performed at room temperature and at 4 °C on unoriented films and oriented fibers of s-PP in the helical or mesomorphic forms. Since the formation of the trans-planar form III is inhibited by stretching at 4 °C s-PP samples in pure mesomorphic form,[18] this study may give new insights into the role that the structural transitions play on the elastic behavior of s-PP.

Experimental Section

Two s-PP samples (sPP1 and sPP2) were synthesized with the single center metallocene catalyst isopropylidene(cyclopentadienyl)(9-fluorenyl)zirconium dichloride, activated with methylalluminoxane according to standard procedure.[20] The fully syndiotactic pentad contents, the molecular weights (M_w), the indices of polydispersity (M_w/M_n), and the melting temperatures of the two samples sPP1 and sPP2 are reported in Table 1.

Unoriented compression-molded films of samples sPP1 and sPP2, crystallized in different forms, were prepared by melting the powder samples in a hot press at 180 °C and cooling the melt in different experimental conditions. Precisely, the samples sPP1A and sPP2A were obtained by cooling the melt to room temperature at cooling rate of about 10 °C/min and are in the crystalline helical form I of s-PP. The samples sPP1B and sPP2B, instead, were obtained by quenching the melt at 0 °C and keeping the samples at 0 °C for 4 and 90 days, respectively, and are crystallized in the pure trans-planar mesomorphic form and in mixtures of helical form I and mesomorphic form, respectively.

Oriented fibers were obtained by stretching at room temperature and at 4 °C films of the samples sPP1B and sPP2B at different values of deformation ϵ ($\epsilon = 100 \times [(L_f - L_i)/L_i]$, with L_f and L_i the final and the initial lengths of the specimen, respectively).

Mechanical tests were performed at room temperature and at 4 °C with a miniature mechanical tester apparatus (MINIMAT by Rheometric Scientific), following the standard test method for tensile properties of thin plastic sheeting ASTM D882-83.

Mechanical tests were first performed on unoriented films of the samples sPP1A, sPP1B, sPP2A, and sPP2B. Rectangular specimens 10 mm long, 5 mm wide, and 0.3 mm thick were stretched up to the break or up to a given strain ϵ at constant deformation rate. Similar tests were then performed on oriented stress-relaxed fibers of the samples sPP1A, sPP1B, sPP2A, and sPP2B. Stress-relaxed fibers were obtained by stretching at room temperature and at 4 °C unoriented films at a given deformation, keeping the fibers under tension for 2 h at the stretching temperature, and then removing the tension allowing the fibers to relax.

The values of the tension set t_s ($t_s = 100 \times [(L_r - L_i)/L_i]$, with L_r the length of the specimen after the relaxation) and the elastic recovery r ($r = 100 \times [(L_f - L_r)/L_r]$) were measured following the recommendation of the standard test method for rubber properties ASTM D412-87.

X-ray diffraction patterns were obtained at room temperature with Ni-filtered Cu Kα radiation. The powder profiles were obtained with an automatic Philips diffractometer, whereas the fiber diffraction patterns were recorded on a BAS-MS imaging plate (FUJIFILM) using a cylindrical camera and processed with a digital imaging reader (FUJIBAS 1800). The X-ray fiber diffraction patterns have been recorded for stretched fibers soon after the stretching and keeping the fibers under tension as well as for relaxed fibers, that is, after keeping the fibers under tension for 2 h and then removing the tension allowing the complete relaxation of the specimens.

The index of crystallinity (x_c) of the unoriented samples was evaluated from the X-ray powder diffraction profiles by the ratio of the crystalline diffraction area and the total area of the diffraction profile.

Results and Discussion

Unoriented Samples. The X-ray powder diffraction profiles of the samples sPP1A, sPP1B, sPP2A, and sPP2B are reported in Figure 1.

The samples sPP1A and sPP2A, obtained by cooling the melt to room temperature at 10 °C/min, are in the helical form I, as indicated by the presence of the 200 and 020 reflections at $2\theta = 12.3°$ and 16°, respectively, in the diffraction profiles a of Figure 1. It is worth noting that the 211 reflection at $2\theta = 18.8°$, typical of a regular alternation of right- and left-handed 2-fold helical chains along both axes of the unit cell of form I,[5] is absent in the diffraction profile of samples sPP2A and very weak in the case of sample sPP1A. This indicates that disordered modifications of form I, characterized by statistical disorder in the positioning of right- and left-handed helical chains in the unit cell,[6] are obtained.

The samples sPP1B and sPP2B have been obtained by quenching the melt at 0 °C and keeping the samples at 0 °C for 4 and 90 days, respectively. The sample sPP1B is in the pure trans-planar mesomorphic form, as indicated by the presence of only two broad peaks at $2\theta = 17$ and 24°, typical of the trans-planar mesomorphic form of s-PP,[15,16] in the diffraction profile b of Figure 1A. The sample sPP2B, instead, is characterized by a mixture of crystals of the trans-planar mesomor-

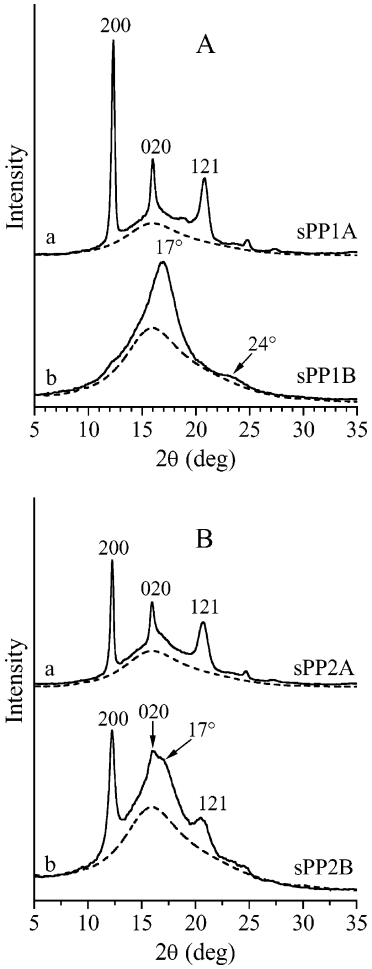

Figure 1. X-ray powder diffraction profiles of the compression-molded films sPP1A and sPP1B of the sample sPP1 with [*rrrr*] = 93% (A) and of the films sPP2A and sPP2B of the sample sPP2 with [*rrrr*] = 78% (B). Dashed lines indicate the diffraction profiles of the amorphous contribution. The 200, 020, and 121 reflections at 2θ = 12.3°, 16°, and 20.9°, respectively, of the helical form I and the broad peaks at 2θ = 17° and 24° of the trans-planar mesomorphic form are indicated. The samples sPP1A and sPP2A are in the helical form I, the sample sPP1B is in the trans-planar mesomorphic form, and the sample sPP2B is in a mixture of the helical form I and the trans-planar mesomorphic form.

phic form and the helical form I, as indicated by the presence of the typical reflections of form I of s-PP and broad peak at 2θ = 17° of the trans-planar mesomorphic form, in the diffraction profile b of Figure 1B.

The different crystallization behavior of the samples sPP1 and sPP2 after quenching at 0 °C is related to the different strereoregularity. It has been recently demonstrated that the formation of the trans-planar mesomorphic form at 0 °C depends on the syndiotacticity of the sample:[17a] the higher the stereoregularity, the faster the formation of the mesomorphic form.[17] For the most stereoregular sample sPP1 ([*rrrr*] = 93%) the residence time of 4 days at 0 °C is enough to stabilize the trans-planar mesomorphic form and inhibit the crystallization of the helical form I at room temperature, whereas for the less stereoregular sample sPP2 ([*rrrr*] = 78%), even very long residence time at 0 °C is not sufficient to stabilize the mesomorphic form and large amounts of crystals of form I are obtained when the sample is removed from the bath at 0 °C and heated to room temperature.

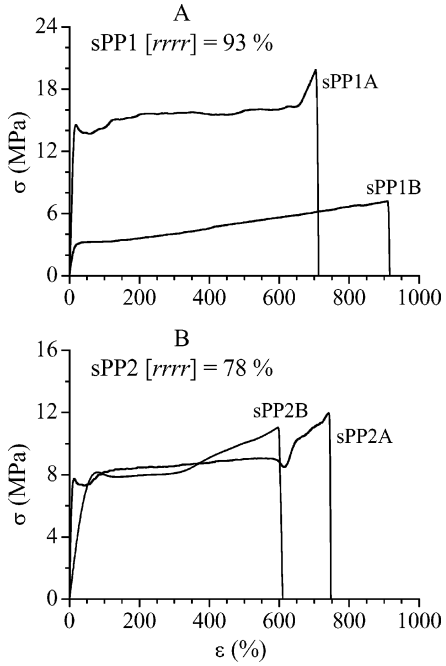

Figure 2. Stress−strain curves recorded at room temperature of unoriented compression-molded films sPP1A and sPP1B of the sample sPP1 with [*rrrr*] = 93% (A) and of the films sPP2A and sPP2B of the sample sPP2 with [*rrrr*] = 78% (B).

The amount of mesomorphic form in the samples sPP1B and sPP2B can be evaluated from the diffraction profiles of Figure 1 considering that the X-ray diffraction profiles arise from the contribution of three different phases: the crystalline helical form I, the trans-planar mesomorphic form, and the amorphous phase, which can be easily separated knowing the diffraction pattern of the three single phases. In particular, the diffraction pattern of the amorphous phase has been obtained from an atactic polypropylene sample, whereas those of the pure trans-planar mesomorphic form and helical form I have been obtained from the sample sPP1 quenched from the melt at 0 °C and kept at 0 °C for long time (>10 days) and few seconds, respectively. Hence, the fractions of the three phases in the samples have been evaluated by the ratios between the area subtending the diffraction profile of the single phase and the area of the whole diffraction profile.

The total fraction of crystalline phase, corresponding to the sum of the amounts of trans-planar mesomorphic form and helical form I, of 30% has been evaluated for both samples sPP1B and sPP2B. It corresponds to the maximum index of crystallinity achievable at room temperature, regardless of the stereoregularity of the sample, the quenching temperature, and the residence time at that temperature.[15,17] The amount of trans-planar mesomorphic form, measured at room temperature as described before, is 30% (100% of the total crystalline phase) for the sample sPP1B and 9% (30% of the total crystalline phase) for the sample sPP2B.

Stress−strain curves recorded at room temperature of the unoriented compression-molded films sPP1A and sPP1B of the most stereoregular sample sPP1, in the helical form I and mesomorphic form, respectively, are reported in Figure 2A. Stress−strain curves recorded at room temperature of the unoriented films sPP2A and sPP2B of the less syndiotactic sample sPP2, crystallized in the helical form I and in a mixture of helical and mesomorphic forms, respectively, are reported in Figure

Table 2. Values of Young's Modulus (E), Stress (σ_b) and Strain (ϵ_b) at Break, and Stress (σ_y) and Strain (ϵ_y) at Yield Point, Measured at Room Temperature, of Unoriented Compression-Molded Films of the Samples sPP1 and sPP2 Crystallized in Helical Form I (sPP1A and sPP2A), in Trans-Planar Mesomorphic Form (sPP1B), and in a Mixture of Form I and Mesomorphic Form (sPP2B)[a]

sample	crystalline form	[*rrrr*] (%)	x_c (%)	E (MPa)	σ_b (MPa)	ϵ_b (%)	σ_y (MPa)	ϵ_y (%)
sPP1A	form I	93	45	251 ± 25	20 ± 5	710 ± 30	14.4	13.4
sPP1B	mesomorphic form	93	30	27 ± 4	7 ± 1	920 ± 40	3.1	20.0
sPP2A	form I	78	35	119 ± 8	12 ± 1	750 ± 20	7.8	16.3
sPP2B	form I + mesomorphic form	78	30	39 ± 5	11 ± 3	620 ± 60	8.1	63.8

[a] The fully syndiotactic pentad contents ([*rrrr*]) and the indices of crystallinity (x_c) of the samples are also reported.

2B. The mechanical properties (Young's modulus, stress and strain at yield point and at break) along with the fully syndiotactic pentad contents and the indices of crystallinity of the unoriented films are reported in Table 2.

It is apparent from Figure 2 and Table 2 that the mechanical properties strongly depend on the crystalline modification of the starting unoriented s-PP film as well as on the stereoregularity of the polymer sample. In fact, for the most stereoregular sample sPP1 ([*rrrr*] = 93%), the values of the Young's modulus and of the stress at any strain of the film sPP1A, crystallized in the helical form I, are much higher than those of the film sPP1B, quenched from the melt at 0 °C and crystallized in pure trans-planar mesomorphic form (Figure 2A and Table 2). This is essentially due to the higher crystallinity of the sample in form I which gives higher rigidity and higher values of elastic modulus. On the other hand, the sample sPP1B, in pure trans-planar mesomorphic form, presents strain at break higher than that of the sample sPP1A, in the crystalline helical form I (Figure 2A). The enhanced ductility of the sample sPP1B with respect to the sample sPP1A is basically related to the different structural organizations: the small and disordered mesomorphic crystals can be, indeed, more easily plastically deformed and with lower strength than the bigger and more ordered crystallites of the helical form I.

Moreover, it is worth noting that, while the sample sPP1B in trans-planar mesomorphic form experiences a homogeneous deformation during stretching up to the break, typical of elastomeric material, the samples sPP1A in helical form I present a different deformation regime, characterized by necking as indicated by the presence of a well-defined yielding in the stress−strain curve of Figure 2A.

In the case of the less stereoregular sample sPP2 ([*rrrr*] = 78%) less differences between the sample sPP2A, crystallized in the helical form I, and the sample sPP2B, crystallized in a mixture of form I and mesomorphic form, are observed. The two samples have, indeed, nearly the same crystallinity and present similar values of strength and deformation at break. However, a lower value of the Young's modulus is observed for the sample sPP2B due to the presence of a nonnegligible amount of disordered mesomorphic crystals (30% of the total crystalline phase).

It is also apparent from Figure 2 and Table 2 that the different syndiotacticity of the samples sPP1 and sPP2 gives different mechanical properties. In fact, both samples sPP1A and sPP2A are slowly crystallized from the melt into the helical form I, but the more stereoregular sample sPP1A presents higher values of Young's modulus and strength due to the higher crystallinity.

In the case of samples sPP1B and sPP2B, quenched from the melt at 0 °C and showing the same crystallinity, the different mechanical behavior is essentially linked to the different amounts of trans-planar mesomorphic form present in the two samples. Although the sample sPP1B is more stereoregular than the sample sPP2B, it shows lower values of the Young's modulus and stress at break because it is crystallized totally in the mesomorphic form. The presence of more ordered crystals of the helical form I (70% of the total crystalline phase) is responsible for the higher rigidity and enhanced strength of the less stereoregular sample sPP2B.

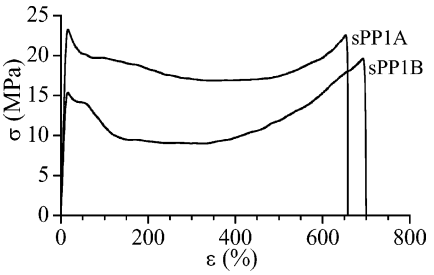

Figure 3. Stress−strain curves recorded at 4 °C of unoriented compression-molded films sPP1A and sPP1B of the sample sPP1 with [*rrrr*] = 93%.

In the case of the most stereoregular sample sPP1 the tensile tests have been also performed at 4 °C. The stress−strain curves recorded at 4 °C of unoriented films of the samples sPP1A and sPP1B are reported in Figure 3. The corresponding values of the mechanical properties are reported in Table 3.

It is apparent that at low temperature for both samples a strong increase of the values of elastic modulus, tensile strength, and stress at any strain and a decrease of the values of strain at break are observed (Table 3). These data are in agreement with the results of ref 3, which have indicated that the values of elastic modulus and tensile strength decrease with increasing the stretching temperature in the range 25−80 °C. The strong increase of the values of elastic modulus of samples sPP1A and sPP1B observed at 4 °C (Table 3) depends on the fact that at this low temperature the samples are very close to the glass transition temperature ($T_g \approx 0$ °C), and the mobility of the molecular chains is strongly reduced.

Moreover, it is worth noting that in the case of the sample sPP1B, in trans-planar mesomorphic form, remarkable differences are observed in the stress−strain curves recorded at 4 °C and at room temperatures. In fact, it is apparent that the homogeneous deformation regime of the sample sPP1B at room temperature (Figure 2A) becomes a necking regime at low temperature, as indicated by the well-defined yielding and the remarkable strain hardening in the stress−strain curve of Figure 3.

The values of tension set ($t_s = 100 \times [(L_r - L_i)/L_i]$) and elastic recovery ($r = 100 \times [(L_f - L_r)/L_r]$), measured at room temperature and at 4 °C, for unoriented films stretched up to 500% and 600% deformation, are

Table 3. Values of Young's Modulus (E), Stress (σ_b) and Strain (ϵ_b) at Break, and Stress (σ_y) and Strain (ϵ_y) at Yield Point, Measured at 4 °C, of Unoriented Films of the Samples sPP1A and sPP1B[a]

sample	crystalline form	[*rrrr*] (%)	x_c (%)	E (MPa)	σ_b (MPa)	ϵ_b (%)	σ_y (MPa)	ϵ_y (%)
sPP1A	form I	93	45	538 ± 50	23 ± 3	655 ± 70	23.3	11.7
sPP1B	mesomorphic form	93	30	72 ± 4	20 ± 3	700 ± 75	15.4	11.8

[a] The fully syndiotactic pentad contents ([*rrrr*]) and the indices of crystallinity (x_c) of the samples are also reported.

Table 4. Values of Tension Set (t_s) and Elastic Recovery (r) Measured at Room Temperature and at 4 °C after Stretching up to 500% or 600% Deformation Unoriented Compression-Molded Films of the Samples sPP1 and sPP2 in the Helical Form I (sPP1A and sPP2A) and in the Mesomorphic Form (sPP1B and sPP2B);[a] Fully Syndiotactic Pentad Contents ([*rrrr*]) of the Samples Are Also Reported

sample	crystalline form	[*rrrr*] (%)	t_s (%) at 25 °C	r (%) at 25 °C	t_s (%) at 4 °C	r (%) at 4 °C
sPP1A	form I	93	275	60	300 (275)[c]	50 (60)[c]
sPP1B	mesomorphic form	93	250	71	367 (250)[c]	28 (71)[c]
sPP2A	form I	78	333[b]	61[b]		
sPP2B	form I + mesomorphic form	78	250	71	300 (250)[c]	50 (71)[c]

[a] Samples of initial length L_i are stretched at 25 or 4 °C up to 500% deformation (final lengths $L_f = 6L_i$), kept in tension at the same temperature for 2 h, and relaxed by releasing the tension. [b] Measured from $\epsilon = 600\%$ ($L_f = 7L_i$). [c] Measured after heating the relaxed fiber to room temperature.

reported in Table 4. These values have been obtained by stretching at room temperature and at 4 °C strips of unoriented s-PP films of initial length L_i up to a final length $L_f = 6L_i$ or $7L_i$ (corresponding to $\epsilon = 500\%$ and 600%, respectively), keeping the fibers in tension for 2 h at the stretching temperature, then removing the tension, and measuring the final length L_r of the relaxed specimen after 10 min at the same temperature.

The high values of tension set of Table 4 indicate that, as already reported in the literature,[2−4] unoriented samples of s-PP of high-medium stereoregularity show poor elastic properties at room temperature, regardless of the crystalline form of the starting unoriented material. Both the unoriented samples sPP1A and sPP2A, in the crystalline helical form I, or the unoriented samples sPP1B and sPP2B, in trans-planar mesomorphic form or in mixtures of crystals of mesomorphic form and form I, experience plastic deformation upon first stretching at room temperature, and only a partial recovery of the initial dimensions is observed upon releasing the tension (Table 4).

The data of Table 4 also indicate that the values of tension set measured at 4 °C for s-PP samples stretched at 4 °C depend on the crystalline modification of the starting unoriented material. In fact, if the crystalline helical form I is present in the unoriented film, the value of tension set at 4 °C is quite similar to that obtained at room temperature (samples sPP1A or sPP2B in Table 4). If the unoriented sample is in pure trans-planar mesomorphic form (sample sPP1B), the tension set measured at 4 °C is higher than that measured at room temperature, indicating that the elastic recovery of the material is further reduced at 4 °C. Moreover, it is worth noting that when s-PP fibers, stretched and relaxed at 4 °C, are heated to room temperature, a further shrinkage of the specimens is observed (Table 4), and the final elastic recovery becomes equal to the value measured at room temperature on fibers stretched at room temperature.

These data can be correlated to the structural analysis reported in past literature[2−4] and in our more recent paper.[18] It has been, indeed, reported that for the s-PP sample with relatively high stereoregularity ([*rrrr*] = 70−80%) stretching procedures at room temperature induce the crystallization of the trans-planar form III, regardless of the crystalline modification of the starting unoriented material. In particular, unoriented samples initially in the helical form I or in the trans-planar mesomorphic form transform, by stretching at room temperature at high deformations, into the trans-planar form III.[2−4,12,18,19] At low stretching temperature (4 °C), instead, the trans-planar form III can be obtained only starting from samples in the helical form I.[18] The mesomorphic form, indeed, does not transform into form III by stretching at 4 °C.[18] Moreover, the removal of the tension in stretched fibers produces structural changes, that depend on the crystalline form of the starting unoriented sample and on the crystalline modifications formed during the stretching.[18]

The X-ray fiber diffraction patterns of fibers of the sample sPP1B, initially in the pure trans-planar mesomorphic form (Figure 1A), stretched at room temperature and at 4 °C at 500% deformation are reported in Figures 4A and 5A, respectively. The corresponding diffraction profiles read along the equatorial line are reported in Figures 4A′ and 5A′, respectively. It is apparent from Figure 4A that the trans-planar mesomorphic form present in the unoriented sample sPP1B transforms into the trans-planar form III by stretching at room temperature, as indicated by the presence of the equatorial $(020)_t$, $(110)_t$, and $(130)_t$ reflections at $2\theta = 16.2°$, 18°, and 29.5°, respectively (Figure 4A′), and the $(021)_t$ and $(111)_t$ reflections on the first layer line (Figure 4A), typical of the trans-planar form III of s-PP.[8] The stretching at 4 °C of the sample sPP1B produces, instead, only orientation of the mesomorphic crystals, as indicated by the presence of the equatorial reflection at $2\theta = 16.7°$ and the broad reflection on the first layer line in the diffraction patterns of Figure 5A,A′.

The X-ray diffraction patterns, and the corresponding equatorial profiles, of the fibers of Figures 4A and 5A after the tension was removed are reported in Figures 4B,B′ and 5B,B′. It is apparent that the trans-planar form III obtained by stretching at room temperature transforms back into the mesomorphic form by releasing the tension, as indicated by the presence of the equatorial reflections at $2\theta \approx 17°$ and 30° of the mesomorphic form in the diffraction pattern of Figure 4B′. No structural transition is, instead, observed by releasing the tension in the fiber in trans-planar mesomorphic form stretched at 4 °C (Figure 5).

This different polymorphic behavior may probably be related to the different mechanical properties shown by the sample sPP1B when stretched at room temperature and at 4 °C. The data of Table 4 and of Figures 4 and 5 indicate, indeed, that when the formation of the trans-

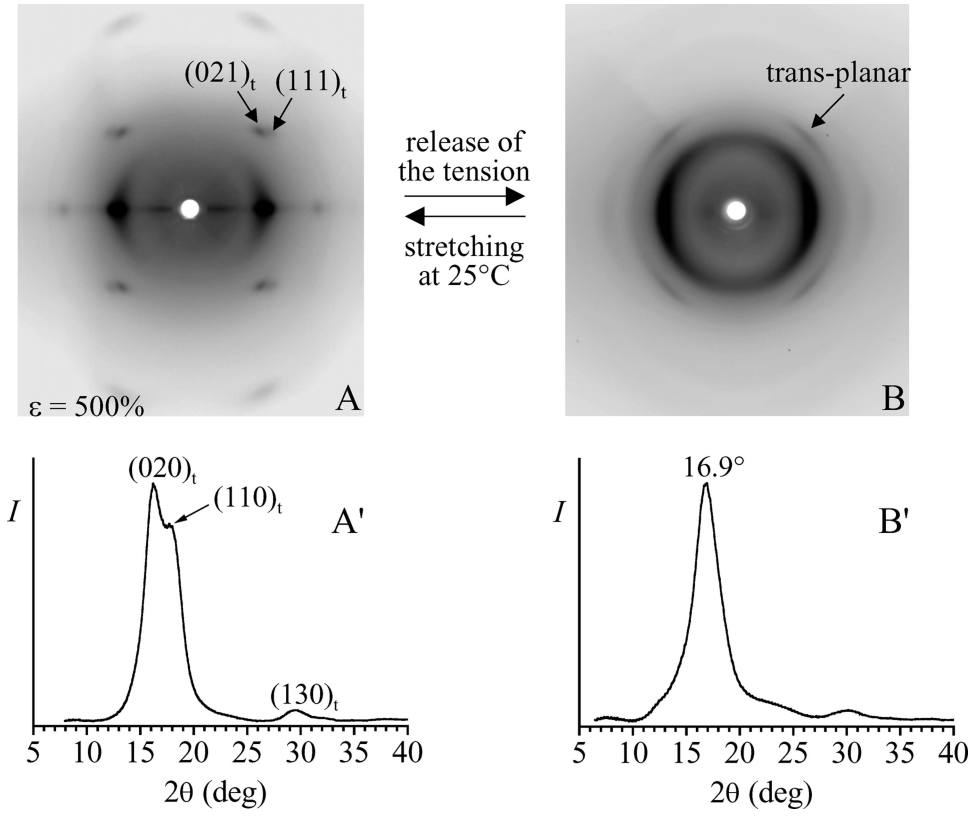

Figure 4. X-ray fiber diffraction patterns (A, B) and corresponding diffraction profiles read along the equator (A′, B′) of fibers obtained by stretching the sample sPP1B at room temperature up to deformation $\epsilon = 500\%$, keeping the fiber in tension (A, A′) and after the tension was removed (B, B′). The $(020)_t$, $(110)_t$, and $(130)_t$ reflections of the trans-planar form III (A′) and the 2θ position of the most intense equatorial peak of the mesomorphic form (B′) are indicated. On the first layer line the reflections arising from the diffraction of crystals of form III ($(021)_t$, $(111)_t$ reflections (A)) and of mesomorphic form (B) are also indicated. The fibers in (A) and (B) are in the form III and mesomorphic form, respectively.

planar form III by stretching is prevented, as in the case of stretching at 4 °C, and no structural transition occurs by releasing the tension (Figure 5), a lower degree of elastic recovery is observed (Table 4).

The X-ray fiber diffraction patterns of fibers of the less stereoregular sample sPP2B, characterized in the unstretched state by a mixture of crystals of the trans-planar mesomorphic form and the helical form I (Figure 1B), stretched at room temperature and at 4 °C are reported in Figures 6A,C and 7A, respectively. It is apparent that, as reported in the literature,[2] for low stereoregular samples the trans-planar form III is obtained at room temperature by stretching only at high deformation ($\epsilon = 600\%$, Figure 6C), whereas at lower deformation fibers in mixtures of crystals of helical form I and mesomorphic form, originally present in the unoriented sPP2B film, are obtained ($\epsilon = 500\%$, Figure 6A). This is shown by the presence of the 200 and 400 reflections of the helical form I and of a quite broad peak at $2\theta = 16.4°$ in the diffraction profile of Figure 6A′. The latter, indeed, arises by the overlapping of the reflection of the trans-planar mesomorphic form ($2\theta = 17°$) and the 020 reflection of the helical form I ($2\theta = 16°$). On the first layer line, reflections corresponding to both the trans-planar and helical chain periodicities are present (Figure 6A). For higher values of deformation ($\epsilon = 600\%$) both crystals of helical form I and trans-planar mesomorphic form transform into the form III, as indicated by the presence of the $(020)_t$, $(110)_t$, and $(130)_t$ reflections of the trans-planar form III in the diffraction profile of Figure 6C′, while the 200 reflection of the helical form I disappears.

When the sample sPP2B is stretched at 4 °C, crystals of the helical form I, initially present in the unoriented film, transform more easily into the trans-planar form III. This is shown in the X-ray diffraction pattern of a fiber of the sample sPP2B stretched at 4 °C up to 500% deformation, reported in Figure 7. In this condition fibers with mixtures of crystals of the helical form I and trans-planar form III are obtained, as indicated by the presence of $(020)_t$, $(110)_t$, $(021)_t$, and $(111)_t$ reflections of the trans-planar form III and the 200 reflection at $2\theta = 12°$ of the helical form (Figure 7A,A′). The high intensity of the reflection at $2\theta = 16°$ is due to the contribution of the $(020)_t$ reflection of form III and the 020 reflection of form I and indicates that the crystals of helical form still present in the oriented fiber correspond to the antichiral form I.[9] The comparison with Figure 6A indicates that the amount of helical form present in the fiber stretched at 4 °C (Figure 7A) is lower than that present in the fiber stretched at room temperature (Figure 6A). Hence, while the stretching at room temperature at 500% deformation basically produces orientation of the crystals of helical form I and trans-planar mesomorphic form (Figure 6A), originally present in the sample sPP2B, with a negligible transition into the form III, the stretching at low temperature produces higher amount of crystals in the trans-planar form, which are mainly in the crystalline form III (Figure 7A). As reported in the literature,[18] these data indicate that at low stretching temperature crystals of form I transform more easily into the trans-planar form III.

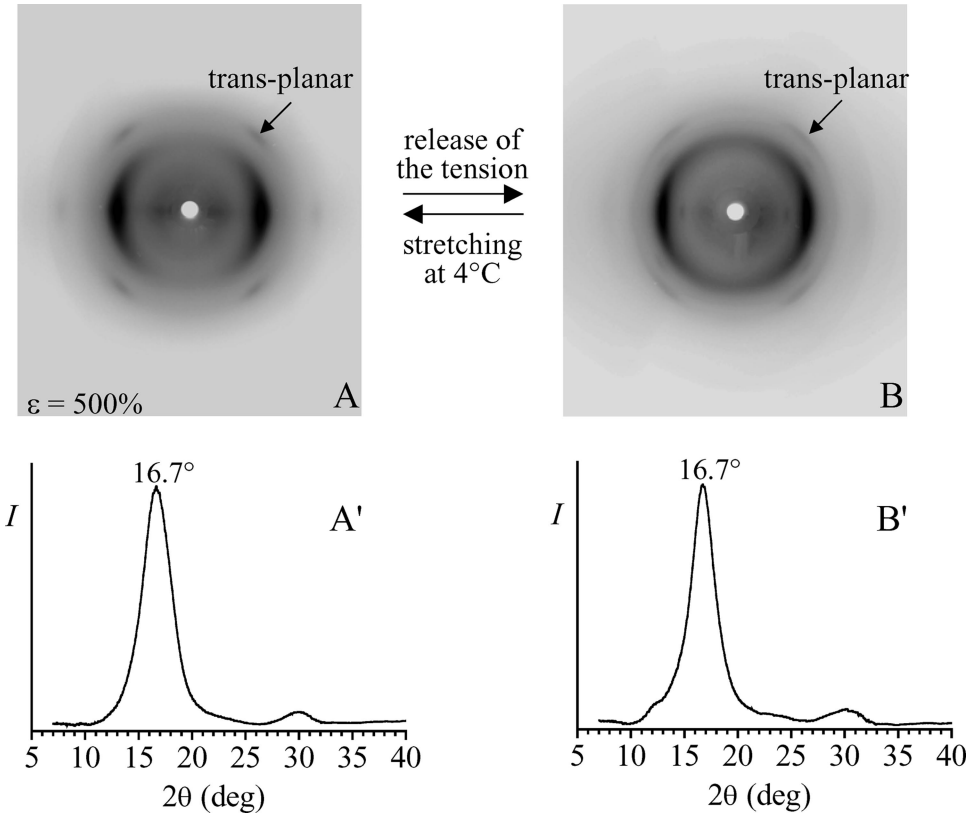

Figure 5. X-ray fiber diffraction patterns (A, B) and corresponding diffraction profiles read along the equator (A′, B′) of fibers obtained by stretching the sample sPP1B at 4 °C up to deformation $\epsilon = 500\%$, keeping the fiber in tension (A, A′) and after the tension was removed (B, B′). The reflections of the trans-planar mesomorphic form are indicated. The fibers in (A) and (B) are in the mesomorphic form.

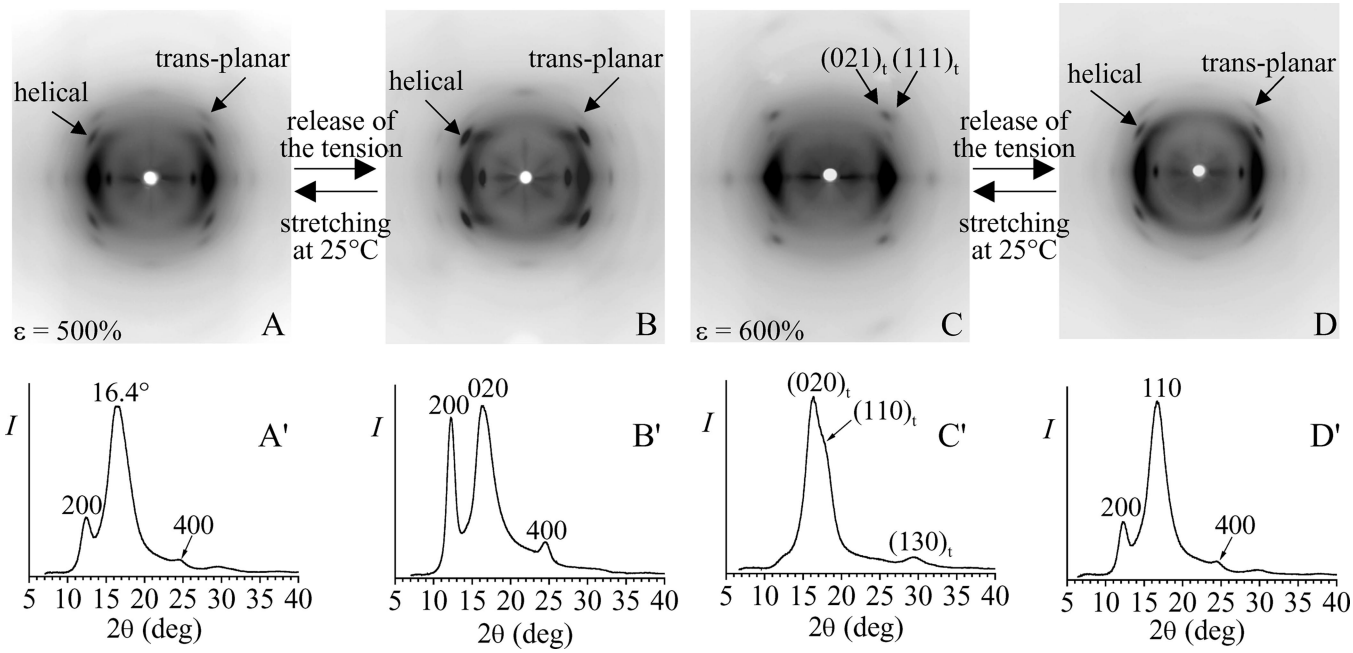

Figure 6. X-ray fiber diffraction patterns (A−D) and corresponding diffraction profiles read along the equator (A′−D′) of fibers obtained by stretching the sample sPP2B at room temperature up to different deformations ϵ, keeping the fiber in tension (A, A′, C, C′) and after the tension was removed (B, B′, D, D′). The 200, 020, and 400 reflections of the antichiral helical form I (A′, B′), the $(020)_t$, $(110)_t$, and $(130)_t$ reflections of the trans-planar form III (C′), and the 110 reflection of the isochiral helical form II (D′) are indicated. On the first layer line reflections arising from the diffraction of crystals of helical and trans-planar mesomorphic forms (A, B, D) and of form III ($(021)_t$, $(111)_t$ reflections (C)) are also indicated. The fibers are in a mixture of form I and mesomorphic form (A), in form I (B), in form III (C), and in a mixture of form II and mesomorphic form (D).

The X-ray fiber diffraction patterns of fibers of Figure 6A,C and 7A after the tension was removed are reported in Figures 6B,D and 7B, respectively.

It is apparent that the release of the tension in the fibers of the sample sPP2B stretched at room temperature at $\epsilon = 500\%$ (Figure 6A) and 600% (Figure 6C)

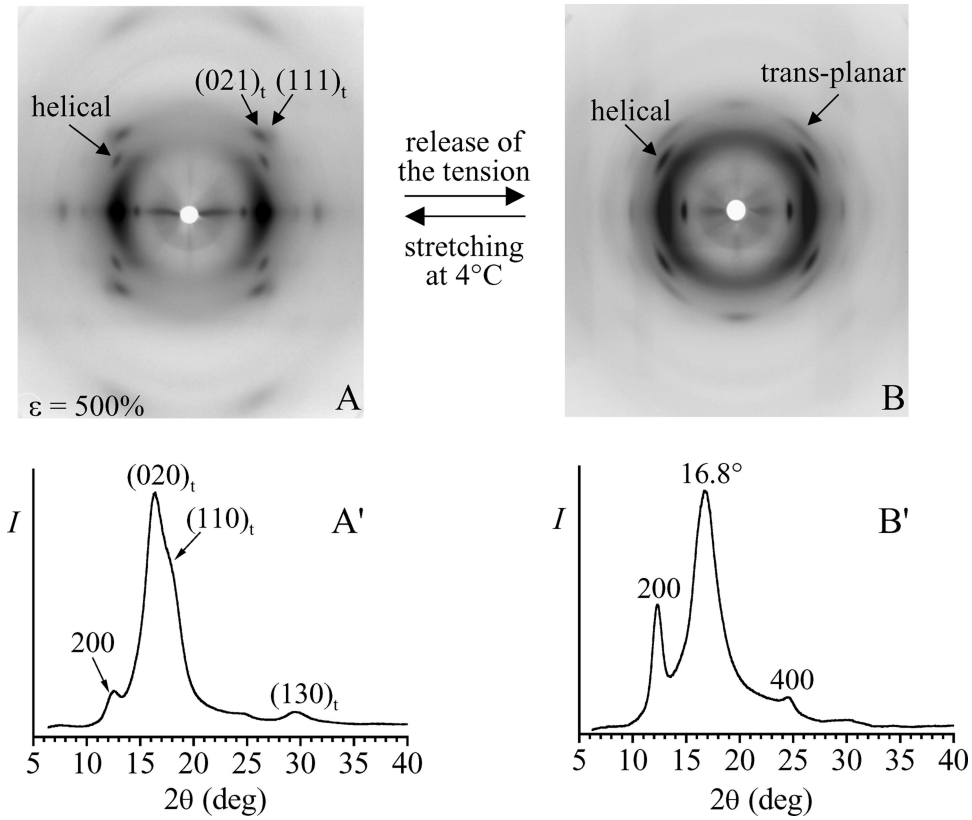

Figure 7. X-ray fiber diffraction patterns (A, B) and corresponding diffraction profiles read along the equator (A′, B′) of fibers obtained by stretching the sample sPP2B at 4 °C up to deformation $\epsilon = 500\%$, keeping the fiber in tension (A, A′) and after the tension was removed (B, B′). The $(020)_t$, $(110)_t$, and $(130)_t$ reflections of the trans-planar form III (A′) and the 200 and 400 reflections of the isochiral helical form II, along with the 2θ position of most intense equatorial peak of the mesomorphic form (B′) are indicated. On the first layer line the reflections arising from the diffraction of crystals of helical form I and form III ($(021)_t$, $(111)_t$ reflections (A)) and trans-planar mesomorphic form (B) are also indicated. The fiber in (A) is in a mixture of form I and form III, whereas the fiber in (B) is in a mixture of form II and mesomorphic form.

gives different results. The fiber relaxed from 500% deformation is basically in the antichiral helical form I, as indicated by the presence of the strong 200 and 020 reflections of form I at $2\theta = 12°$ and 16°, respectively, in the diffraction pattern of Figure 6B,B′. However, the presence of reflections on the first layer line corresponding to the chain periodicity of 5.1 Å (Figure 6B) indicates that a small fraction of crystal in trans-planar conformation, likely in mesomorphic form, is present in the fiber. When the fiber is relaxed from 600% deformation, instead, a mixture of the isochiral helical form II and the trans-planar mesomorphic form is obtained, as indicated by the presence of the 200 and 110 reflections at $2\theta = 12.3°$ and 17°, typical of form II, and reflections on the first layer line corresponding to the trans-planar chain periodicity in the pattern of Figure 6D,D′.

A similar result is obtained after removing the tension in fibers of the sample sPP2B stretched at 4 °C (Figure 7). As shown in Figure 7B, the trans-planar form III present in the stretched fiber (Figure 7A) transforms into a mixture of helical form II and trans-planar mesomorphic form upon releasing the tension.

These data further confirm the hypothesis recently reported in the literature that the structural evolution of the trans-planar form III upon removing the tension in stretched fibers depends on the memory of the crystalline forms present in the starting unoriented material[18] and that the formation of the isochiral helical form II of s-PP is strictly related to that of the trans-planar form III.[3,12−14] Moreover, the similar polymorphic behavior of the sample sPP2B, in a mixture of helical form I and trans-planar mesomorphic form, upon relaxation from fibers stretched at room temperature (Figure 6) and at 4 °C (Figure 7) is related to the similar elastic recovery experienced by the fibers at room temperature and at 4 °C (Table 4). In fact, crystalline phase transitions occur upon removing the tension, regardless of the stretching temperature. The trans-planar mesomorphic form transforms into the helical form I upon relaxation from stretching at room temperature (Figure 6A,B), and the trans-planar form III transforms into the helical form II upon relaxation from stretching at 4 °C (Figure 7) or at room temperature at higher deformation (Figure 6C,D).

Oriented Samples. The mechanical tests have been also performed on stress-relaxed fibers of the samples sPP1 and sPP2. These fibers were prepared by stretching at room temperature the samples sPP1A, sPP1B, and sPP2B up to 500% deformation, and the sample sPP2A up to 600% deformation, keeping the fibers under tension at the same temperature for 2 h, and then removing the tension, allowing the specimens to relax. (The fibers stress-relaxed from 500% deformation are identified as sPP1A-500, sPP1B-500, and sPP2B-500, whereas the fiber of the sample sPP2A stress-relaxed from 600% deformation is identified as sPP2A-600.) The less stereoregular sample sPP2A has been stretched at higher deformation in order to obtain a fiber in trans-planar form III.

As discussed in the previous section, the stress-relaxed fibers sPP1B-500 and sPP2B-500 are in the

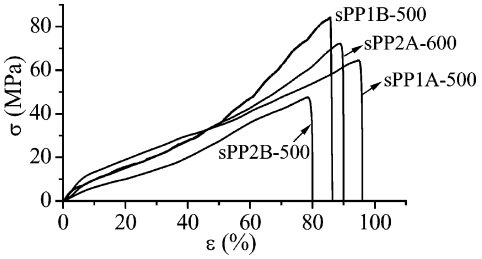

Figure 8. Stress−strain curves recorded at room temperature of strained and stress-relaxed fibers sPP1A-500, sPP1B-500, sPP2A-600, and sPP2B-500. The fibers have been obtained by stretching at room temperature unoriented films of the samples sPP1A, sPP1B, and sPP2B up to 500% deformation, keeping the fibers under tension at room temperature for 2 h and then removing the tension. For the sample sPP2A the stress−strain curve of a fiber stress-relaxed from 600% deformation is reported.

Table 5. Values of Young's Modulus (E), Stress (σ_b) and Strain (ϵ_b) at Break, Measured at Room Temperature, of Stress-Relaxed Fibers of the Samples sPP1 and sPP2;[a] Fully Syndiotactic Pentad Contents ([*rrrr*]) of the Samples Are Also Reported

sample	crystalline form	[*rrrr*] (%)	E (MPa)	σ_b (MPa)	ϵ_b (%)
sPP1A-500	form II	93	254 ± 6	60 ± 8	96 ± 10
sPP1B-500	mesomorphic form	93	132 ± 20	84 ± 2	85 ± 3
sPP2A-600[b]	form II	78	167 ± 10	72 ± 2	90 ± 5
sPP2B-500	form I	78	67 ± 3	44 ± 2	80 ± 6

[a] The stress-relaxed fibers were prepared by stretching at 25 °C up to 500% deformation samples of initial length L_i (final lengths $L_f = 6L_i$), keeping the fibers in tension at the same temperature for 2 h, then removing the tension allowing the specimens to relax. [b] For this sample the fiber was stress-relaxed from $\epsilon = 600\%$ ($L_f = 7L_i$).

trans-planar mesomorphic form (Figures 4B,B′) and mainly in the helical form I (Figures 6B,B′), respectively, whereas the stress-relaxed fibers sPP1A-500 and sPP2A-600 are in the isochiral helical form II.[2,3,12]

The stress−strain curves recorded at room temperature of these stress-relaxed fibers are reported in Figure 8. The corresponding mechanical properties are reported in Table 5.

All the fibers present similar stress−strain curves with comparable values of the stress and strain at break (Figure 8 and Table 5). Substantial differences are observed only in the values of Young's modulus which, as occurs for the unoriented films (Table 2), are essentially related to the stereoregularity and the crystalline modification of the relaxed fibers. The values of elastic modulus of fibers of the more stereoregular samples sPP1A and sPP1B are higher than those of fibers of the less stereoregular samples sPP2A and sPP2B, respectively (Table 5). On the other hand, for both samples sPP1 and sPP2, fibers sPP1A-500 and sPP2A-600 in the helical form II show values of elastic modulus higher than those of fibers sPP1B-500 and sPP2B-500 in the trans-planar mesomorphic form (Figure 4B) and in a mixture of crystals of the mesomorphic form and the helical form I (Figure 6B), respectively (Table 5).

Moreover, in agreement with the literature,[2,3,13,14] the tensile behavior of oriented fibers of s-PP is different from that of unoriented samples. In fact, while unoriented films present stress−strain curves typical of thermoplastic materials (Figure 2), oriented fibers show

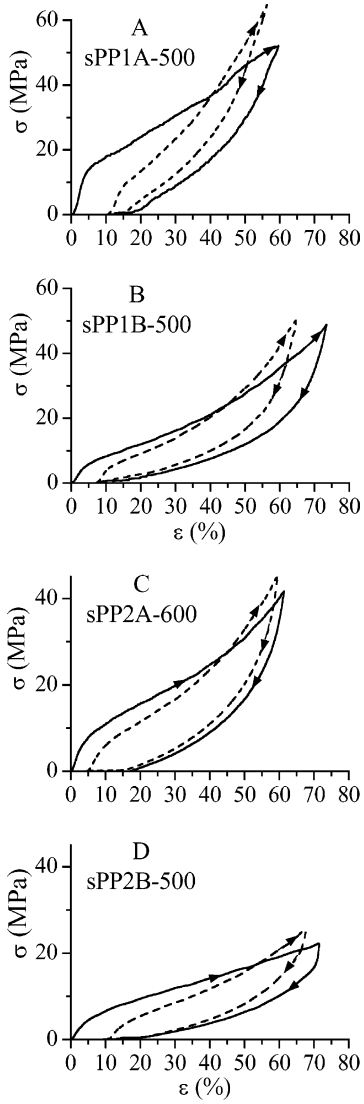

Figure 9. Stress−strain hysteresis cycles recorded at room temperature, composed of the stretching and relaxation steps according to the directions of the arrows, of strained and stress-relaxed fibers of the samples sPP1 and sPP2. Fibers sPP1A-500 (A), sPP1B-500 (B), and sPP2B-500 (D) are stress-relaxed from fibers of the samples sPP1A, sPP1B, and sPP2B, respectively, stretched at room temperature up to 500% deformation. The fiber sPP2A-600 (C) is stress-relaxed from fibers of the sample sPP2A stretched at room temperature up to 600% deformation. The first hysteresis cycles (solid lines) and curves averaged over three consecutive cycles successive to the first one (dashed lines) are reported.

stress−strain curves typical of elastomers, with small yielding and remarkable strain hardening (Figure 8).

To quantify the elastic properties of the oriented fibers, hysteresis cycles have been performed at room temperature on the stress-relaxed fibers of the samples sPP1 and sPP2. The hysteresis cycles composed of the stress−strain curves measured during the stretching, immediately followed by stress−strain curves measured during relaxation, are reported in Figure 9. In these cycles, stress-relaxed fibers of the new initial length L_r are stretched up to the final length L_f ($L_f = 6L_i$ for the fibers sPP1A-500, sPP1B-500, and sPP2B-500, whereas $L_f = 7L_i$ for the fiber sPP2A-600), that is, up to a maximum strain (ϵ_{max}) numerically coincident with the value of elastic recovery reported in Table 4. The value of maximum strain was chosen in order to avoid further plastic deformation of the fibers during the stretching

Table 6. Values of Maximum Strain (ϵ_{max}), Tension Set (t_s), and Dissipated Energy (E_{diss}) Measured in the Hysteresis Cycles of Figure 9 Recorded at Room Temperature for Stress-Relaxed Fibers of the Samples sPP1 and sPP2

sample	ϵ_{max} (%) (I cycle)	t_s (%) (I cycle)	E_{diss} (%) (I cycle)	ϵ_{max} (%) (II cycle)	t_s (%) (II cycle)	ϵ_{max} (%) (III−V cycles)	t_s (%) (III−V cycles)	$\langle E_{diss}\rangle^a$ (%) (II−V cycle)
sPP1A-500	60	9.3	56	46	2.4	43	0	33
sPP1B-500	71	6.3	54	61	1.7	58	0	42
sPP2A-600	61	4.6	61	54	0	54	0	50
sPP2B-500	71	9.5	64	56	2.5	52	0	48

[a] Averaged over the values measured in the consecutive hysteresis cycles successive to the first one.

step of the hysteresis cycles.

For each fiber at least four consecutive hysteresis cycles were recorded: each cycle was performed 10 min after the end of the previous cycle. The values of maximum strain, tension set, and dissipated energy measured after each cycle are reported in Table 6. For all the stress-relaxed fibers the values of tension set, measured after the first hysteresis cycle, are very low (<10%) and become close to zero starting from the second cycle, the successive hysteresis cycles recorded after the first one being all nearly coincident (Figure 9 and Table 6).

The data of Figure 9 and Table 6 indicate that, despite the different structural organization, oriented fibers of s-PP present good elastic properties at room temperature with total recovery of the initial dimensions in a deformation range of 40−60%. For all fibers of Figure 9 the elastic recovery is associated with a reversible polymorphic transition occurring during successive mechanical cycles of stretching and relaxation. In the case of fiber sPP1A-500 (Figure 9A) and sPP2A-600 (Figure 9C), the reversible transition between the helical form II and the trans-planar form III occurs during cycles, whereas the transition between the trans-planar mesomorphic form and the trans-planar form III occurs for the fiber sPP1B-500 (Figures 4 and 9B), and finally, the transition between the helical form I and the trans-planar mesomorphic form occurs for the fiber sPP2B-500 (Figures 6A,B and 9D).

As shown in Figures 5 and 7, oriented fibers have been also obtained by stretching at 4 °C; therefore, hysteresis cycles have been also performed at 4 °C. The fibers were prepared by stretching at 4 °C the samples sPP1A, sPP1B, and sPP2B up to 500% deformation, keeping the fibers in tension for 2 h at 4 °C, and then removing the tension at 4 °C. These stress-relaxed fibers are identified as sPP1A4-500, sPP1B4-500, and sPP2B4-500 and have been analyzed at room temperature by X-ray diffraction and are in the helical form II, in the trans-planar mesomorphic form (Figure 5B), and in mixture of the helical form II and trans-planar mesomorphic form (Figure 7B), respectively. The hysteresis cycles recorded at 4 °C of the fibers sPP1A4-500, sPP1B4-500, and sPP2B4-500 are reported in Figure 10. The values of maximum strain, tension set, and dissipated energy measured after each cycle are reported in Table 7. The values of maximum strains achieved in the first hysteresis cycles of Figure 10, reported in Table 7, are numerically coincident with the values of elastic recovery measured for each fiber at room temperature and reported in Table 4.

The data of Figure 10 and Table 7 indicate that, while fibers of the samples sPP1A and sPP2B stretched at room temperature and at 4 °C (fibers sPP1A-500 and sPP1A4-500 and fibers sPP2B-500 and sPP2B4-500) show similar hysteresis cycles with similar values of tension set, for stress-relaxed fibers of the sample sPP1B a different behavior is observed. In particular, for the

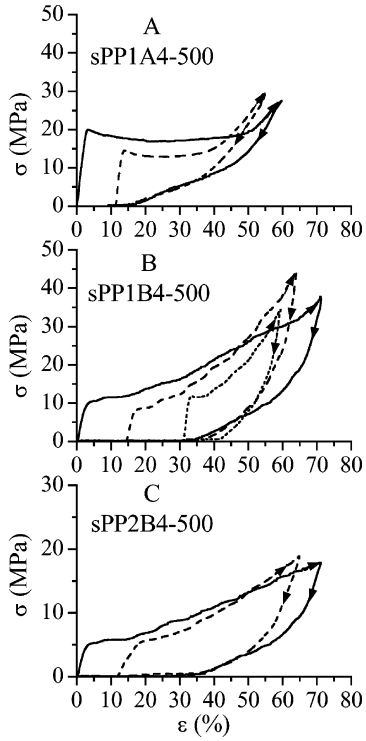

Figure 10. Stress−strain hysteresis cycles recorded at 4 °C, composed of the stretching and relaxation steps according to the directions of the arrows, of strained and stress-relaxed fibers of the samples sPP1 and sPP2. Fibers sPP1A4-500 (A), sPP1B4-500 (B), and sPP2B4-500 (C) are stress-relaxed from fibers of the samples sPP1A, sPP1B, and sPP2B, respectively, stretched at 4 °C up to 500% deformation. In (A) and (C) the first hysteresis cycles (solid lines) and curves averaged over three consecutive cycles successive to the first one (dashed lines) are reported. In (B) the first (solid line) and the second (dashed line) hysteresis cycles and curves averaged over three consecutive cycles successive to the second one (dotted lines) are reported.

stress-relaxed fibers sPP1A4-500 and sPP2B4-500 the values of tension set and dissipated energy involved in the hysteresis cycles at 4 °C (Table 7) are similar to those measured at room temperature (Table 6). Moreover, as occurs at room temperature, consecutive hysteresis cycles successive to the first one are nearly coincident, the residual tension set being nearly zero (Figure 10A,C and Table 7). This indicates that these fibers present a good elastic behavior also at 4 °C in a large deformation range, almost equal to that obtained at room temperature (Tables 6 and 7).

For the fiber of the sample sPP1B stretched at 4 °C (fiber sPP1B4-500), instead, the value of tension set measured at 4 °C after the first hysteresis cycle is greater than that measured at room temperature (fiber sPP1B-500), and a further increase is observed after the second cycle (Tables 6 and 7 and Figure 10B). Only starting from the third cycle the residual set is close to zero, consecutive cycles successive to the second one

Table 7. Values of Maximum Strain (ϵ_{max}), Tension Set (t_s), and Dissipated Energy (E_{diss}) Measured in the Hysteresis Cycles of Figure 10 Recorded at 4 °C for Stress-Relaxed Fibers of the Samples sPP1 and sPP2

sample	ϵ_{max} (%) (I cycle)	t_s (%) (I cycle)	E_{diss} (%) (I cycle)	ϵ_{max} (%) (II cycle)	t_s (%) (II cycle)	E_{diss} (%) (II cycle)	ϵ_{max} (%) (III−V cycles)	t_s (%) (III−V cycles)	E_{diss} (%) (III−V cycles)
sPP1A4-500	60	9.3	62	46	3.7	47	41	0	40
sPP1B4-500	71	14.2	72	50	16.7	68	28	0	62
sPP2B4-500	71	9.5	72	56	4.3	72	50	0	64

being all nearly coincident (Figure 10B). This indicates that for the fiber sPP1B4-500 the elastic behavior observed at room temperature is extremely reduced at 4 °C, being preserved only in a very small deformation range (28% compared to the deformation range of 60% obtained at room temperature).

The different elastic behavior at 4 °C depends essentially on the different structural organizations of the s-PP fibers and may be rationalized on the basis on the structural analysis reported in the previous section. At 4 °C, in the case of the fibers sPP1A4-500 and sPP2B4-500, the observed elastic behavior (Figure 10A,C and Table 7) is associated with reversible polymorphic transitions occurring during the stretching and relaxation cycles. In particular, for the stress-relaxed fiber sPP1A4-500, initially in the helical form II, a reversible transition between the trans-planar form III, formed during stretching, and the helical form II occurs during the mechanical cycles. For the stress-relaxed fiber sPP2B4-500, initially in a mixture of the trans-planar mesomorphic form and the helical form II (Figure 7B), similar reversible transition between the trans-planar form III and the helical form II occurs during the stretching relaxation cycles (Figure 7). No structural transition, instead, occurs during the stretching relaxation cycles of the fiber sPP1B4-500 (Figure 5), and correspondingly, a reduced elastic behavior is observed (Figure 10B and Table 7).

Stress-relaxed fibers of the sample sPP1B, originally in the pure trans-planar mesomorphic form (Figure 1A), are always in mesomorphic form, whatever the temperature at which the stretching is performed (Figures 4B and 5B). When such fibers are stretched again at room temperature, the mesomorphic form transforms into the trans-planar form III (Figure 4A) and a good elastic behavior is observed (Figure 9B). When the stretching is performed at 4 °C, instead, the mesomorphic form does not transforms into form III by stretching, no structural transition occurs upon removing the tension (Figure 5), and correspondingly, an elastic behavior in a very small deformation range is observed (Figure 10B). These results support the hypothesis that the elasticity of oriented fibers of s-PP is not merely entropic, as in conventional elastomers, but is also due to an enthalpic effect, being strictly related to the structural transitions occurring in the crystalline regions. The entropic effect, due to the conformational transitions of the amorphous chains, which connect as tie chains the crystalline domains, and the enthalpic contribution, due to the metastability of the trans-planar form III, which transforms into modifications more stable in the unstretched state, act in synergy and simultaneously producing the elastic recovery in both crystalline and mesomorphic s-PP.

Conclusions

The mechanical properties of s-PP samples with different stereoregularity and crystallized in helical form I and in trans-planar mesomorphic form have been analyzed. Unoriented samples of high-medium stereoregularity ([*rrrr*] = 78−93%) show poor elastic properties at room temperature, regardless of the starting crystalline forms. Both the helical and trans-planar mesomorphic forms of s-PP experience by stretching at room temperature irreversible plastic deformation and only a small recovery of the initial dimensions of the specimens is observed upon removing the tension. At low temperature (4 °C) the mechanical properties depend, instead, on the crystalline form of the unoriented sample. In fact, while crystalline samples of s-PP in the helical form I show similar behavior at room temperature and at 4 °C, for samples in the trans-planar mesomorphic form the elastic recovery of the material is further reduced when the stretching is performed at 4 °C.

Oriented fibers of s-PP show good elastic properties at room temperature in deformation ranges of 40−60%, regardless of the crystalline form of the starting fiber. At 4 °C the elastic behavior depends, instead, on the crystalline modifications present in the oriented fiber. If the fiber is initially in the helical form I or form II, the elastic properties are maintained at low temperature and the values of elastic recovery are similar to those observed at room temperature. If the fiber is, instead, in the trans-planar mesomorphic form, the elastic recovery is significantly reduced.

The observed mechanical behavior is related to the structural organization and polymorphic transformations occurring during stretching and relaxation. The elastic behavior observed at room temperature and at 4 °C is, indeed, associated with reversible phase transitions between the trans-planar forms and the more stable helical modifications of s-PP, occurring during successive stretching and relaxation of fibers. When the structural transition does not occur, as in the case of fibers in pure trans-planar mesomorphic form stretched at 4 °C, the elastic properties are significantly reduced in a very small deformation range.

These results clearly indicate that the elasticity of fibers of s-PP is also due to an enthalpic contribution, being related to the phase transitions occurring in the crystalline regions. A good elastic behavior is, indeed, observed also at 4 °C, but only when crystalline phase transitions occur upon removing the tension. However, since a small elastic recovery is observed at 4 °C, also in absence of phase transition, the entropic effect due to the conformational transition of the amorphous chains, which connect as tie chains the crystalline domains, gives a contribution to the elasticity of s-PP as in conventional elastomers. The enthalpic and entropic effects act simultaneously, producing elastic recovery in crystalline and mesomorphic s-PP fibers.

Acknowledgment. Financial support from the "Ministero dell'Istruzione, dell'Università e della Ricerca" (PRIN 2002 and Cluster C26 projects) is gratefully acknowledged.

References and Notes

(1) (a) Loos, J.; Huckert, A.; Petermann, J. *Colloid Polym. Sci.* **1996**, *274*, 100. (b) Loos, J.; Schimanski, T. *Polym. Eng. Sci.* **2000**, *40*, 567.

(2) Auriemma, F.; Ruiz de Ballesteros, O.; De Rosa, C. *Macromolecules* **2001**, *34*, 4485.

(3) De Rosa, C.; Gargiulo, M. C.; Auriemma, F.; Ruiz de Ballesteros, O.; Razavi, A. *Macromolecules* **2002**, *35*, 9083.

(4) (a) D'Aniello, C.; Guadagno, L.; Naddeo, C.; Vittoria, V. *Macromol. Rapid Commun.* **2001**, *22*, 104. (b) Guadagno, L.; D'Aniello, C.; Naddeo, C.; Vittoria, V. *Macromolecules* **2001**, *34*, 2512. (c) Guadagno, L.; D'Aniello, C.; Naddeo, C.; Vittoria, V.; Meille, S. V. *Macromolecules* **2002**, *35*, 3921.

(5) Lotz, B.; Lovinger, A. J.; Cais, R. E. *Macromolecules* **1988**, *21*, 2375.

(6) De Rosa, C.; Auriemma, F.; Vinti, V. *Macromolecules* **1997**, *30*, 4137.

(7) Natta, G.; Peraldo, M.; Allegra, G. *Makromol. Chem.* **1964**, *75*, 215.

(8) Chatani, Y.; Maruyama, H.; Noguchi, K.; Asanuma, T.; Shiomura, T. *J. Polym. Sci., Part C* **1990**, *28*, 393.

(9) De Rosa, C.; Corradini, P. *Macromolecules* **1993**, *26*, 5711.

(10) De Rosa, C.; Auriemma, F.; Vinti, V. *Macromolecules* **1998**, *31*, 7430.

(11) Corradini, P.; Natta, G.; Ganis, P.; Temussi, P. A. *J. Polym. Sci., Part C* **1967**, *16*, 2477.

(12) (a) Auriemma, F.; De Rosa, C. *J. Am. Chem. Soc.* **2003**, *125*, 13143. (b) Auriemma, F.; De Rosa, C. *Macromolecules*, **2003**, *36*, 9396.

(13) De Rosa, C.; Auriemma, F.; Ruiz de Ballesteros, O.; Resconi, L.; Fait, A.; Ciaccia, E.; Camurati, I. *J. Am. Chem. Soc.* **2003**, *125*, 10913.

(14) (a) De Rosa, C.; Auriemma, F.; Ruiz de Ballesteros, O. *Macromolecules* **2003**, *36*, 7607. (b) De Rosa, C.; Auriemma, F.; Ruiz de Ballesteros, O. *Macromolecules* **2004**, *37*, 1422.

(15) (a) Nakaoki, T.; Ohira, Y.; Hayashi, H.; Horii, F. *Macromolecules* **1998**, *31*, 2705. (b) Ohira, Y.; Horii, F.; Nakaoki, T. *Macromolecules* **2000**, *33*, 1801. (c) Ohira, Y.; Horii, F.; Nakaoki, T. *Macromolecules* **2001**, *34*, 1655. (d) Ohira, Y.; Horii, F.; Nakaoki, T. *Macromolecules* **2000**, *33*, 5566.

(16) Vittoria, V.; Guadagno, L.; Comotti, A.; Simonutti, R.; Auriemma, F.; De Rosa, C. *Macromolecules* **2000**, *33*, 6200.

(17) (a) De Rosa, C.; Auriemma, F.; Ruiz de Ballesteros, O. *Polymer* **2001**, *42*, 9729. (b) De Rosa, C.; Ruiz de Ballesteros, O.; Santoro, M.; Auriemma, F. *Polymer* **2003**, *44*, 6267.

(18) De Rosa, C.; Ruiz de Ballesteros, O.; Santoro, M.; Auriemma, F. *Macromolecules* **2004**, *37*, 1816.

(19) Guadagno, L.; D'Aniello, C.; Naddeo, C.; Vittoria, V. *Macromolecules* **2000**, *33*, 6023. (b) Guadagno, L.; D'Aniello, C.; Naddeo, C.; Vittoria, V.; Meille, S. V. *Macromolecules* **2003**, *36*, 6756.

(20) Ewen, J. A.; Jones, R.; Razavi, A.; Ferrara, J. D. *J. Am. Chem. Soc.* **1988**, *110*, 6255.

MA049214H